ELSEVIER

Journal of Alloys and Compounds 224 (1995) 60–65

Journal of ALLOYS AND COMPOUNDS

X-ray and time differential perturbed angular correlation measurements in $ZrCr_2$ and $ZrCr_2H_3$ Laves phase compounds

J. Mestnik Filho, A.W. Carbonari, W. Pendl Jr., J.I. Moura, R.N. Saxena

Instituto de Pesquisas Energéticas e Nucleares, IPEN-CNEN/SP, Cx. Postal 11049, 0.5422-970 São Paulo SP, Brazil

Received 7 October 1994

Abstract

The existence of stacking defects in $ZrCr_2$ has been detected by X-ray analysis and the time differential perturbed angular correlation (TDPAC) technique, using ^{181}Ta probes occupying Zr sites. It was found that two types of Zr site are responsible for the large observed width of the distribution of electric field gradient (EFG) at the ^{181}Ta probes. One type of Zr site is the normal $P6_3/mmc$ lattice position which possesses $3m$ point symmetry. The other zirconium site comes from stacking defect positions which relax to a local configuration with $\bar{4}3m$ point symmetry, thus generating strains around the defects. The mean EFG and its asymmetry parameter η for $ZrCr_2$ are temperature independent in the range $77 \leqslant T \leqslant 300$ K, while for $ZrCr_2H_3$ a phase transition occurs at 230 K. This phase transition is quite wide and ranges from 200 to 260 K.

Keywords: Laves phase; Metal hydrides; Crystal defects; TDPAC measurements; X-ray measurements

1. Introduction

The $ZrCr_2$ intermetallic compound belongs to a group of metallic structures known as AB_2 Laves phases which have peculiar properties when hydrogen is added to form a ternary system. Quite frequently the element A is a strong hydrogen absorber such as Ti, Zr, Hf or a rare earth element, whereas the element B may be another hydrogen absorber from a different group in the periodic table, e.g. V, or an element without appreciable affinity towards hydrogen such as Cr, Mn or Fe. Appropriate amounts of these elements may be adjusted in order that the Laves phase formed presents hydrogen absorption–desorption characteristics which are adequate for a particular application.

Laves phases which absorb hydrogen have recently been studied with respect to the preference of occupation of the different interstitial sites by hydrogen atoms [1–3]. Since these compounds present various kinds of available sites for hydrogen occupation, they are suitable for testing theoretical predictions of site occupation [4,5].

The time differential perturbed angular correlation (TDPAC) technique is a potential tool for observing the effects caused by the hydrogen atoms in metal hydrides, especially in compounds in which the standard probe nucleus ^{181}Ta occupies the known sites in substitution of Zr or Hf. Since the nuclear state of the probe is perturbed by the environmental electric field gradient, the presence of hydrogen atoms can be detected by the changes they can cause in these crystalline fields, especially for slow-moving hydrogen atoms at low concentrations.

In the present work we have carried out TDPAC measurements on $ZrCr_2$ and its hydride and detect a structural stacking defect in the alloy which limits the observation of the effects caused by hydrogen at low concentrations. A structural analysis of the Zr sites around the defects, based on refined X-ray powder diffraction data, is presented.

2. Preparation of the samples

The $ZrCr_2$ compound was prepared by melting the constituent elements in an arc furnace under an argon atmosphere. The quoted purity of the starting elements was better than 99.5%. For the TDPAC samples approximately 0.1 at.% of zirconium was substituted by hafnium previously irradiated with neutrons in the IEA-R1 reactor.

The hydrogenation of $ZrCr_2$ was carried out in a standard Sievert-type facility in which the required amount of hydrogen gas is trapped in a calibrated volume before the chemical absorption reaction. The sample was submitted to a degassing process under

SSDI 0925-8388(95)01513-2

vacuum at 653 K until the pressure inside the stainless steel sample holder attained 10^{-6} mbar. In the first cycle of hydrogenation the sample was submitted to 20 bar of hydrogen gas at room temperature. After the completion of the chemical reaction, the hydrogen gas inside the vessel was removed and the temperature of the sample was raised to 873 K in order to allow it to desorb hydrogen under vacuum. In the second cycle, after the sample had absorbed the required amount of hydrogen, it was cooled to liquid nitrogen temperature and then allowed to react with oxygen at 0.4 bar for about 3 h. After that, the fine powdered sample could be exposed to air without burning. The hydrogenation of the samples has been carried out after purifying the hydrogen gas. The gas purification was accomplished by absorbing and desorbing hydrogen gas by titanium sponge prior to the absorption by the $ZrCr_2$ alloy.

3. The structure of $ZrCr_2$

There is some controversy in the literature concerning the structure of the $ZrCr_2$ compound. For example, Rostoker [6] reported a C14 hexagonal Laves phase [7] type of structure, space group $P6_3/mmc$, for $ZrCr_2$ at temperatures below 900 °C and a C15 cubic Laves phase type of structure, space group $Fd3m$, for temperatures above 994 °C. Fruchart et al. [8] and Riesterer et al. [9] reported the cubic structure at room temperature, whereas Ivey and Northwood [10] found the hexagonal C14 Laves phase type under the same conditions.

The X-ray powder diffraction pattern (Cu Kα radiation) for $ZrCr_2$ obtained in this work is shown in Fig. 1. A similar pattern, not shown here, is obtained for the hydride $ZrCr_2H_3$, but the diffraction lines are somewhat broader for this case. The diffraction patterns are consistent with a hexagonal C14 structure, thus in agreement with Rostoker [6] and Ivey and Northwood [10]. A structure refinement by the Rietveld method [11] confirmed the C14 structure type but also revealed the presence of other phases. The results of the refinement are shown in Fig. 1 and Table 1. The following features were observed. (1) There are two small peaks, marked with arrows in Fig. 1, at the positions $2\theta = 33.67°$ and 38.71° which are not reflections of the refined structure. (2) The intensities of some of the diffraction lines are not well reproduced in the refinement, as can be seen in the difference profile at the bottom of Fig. 1.

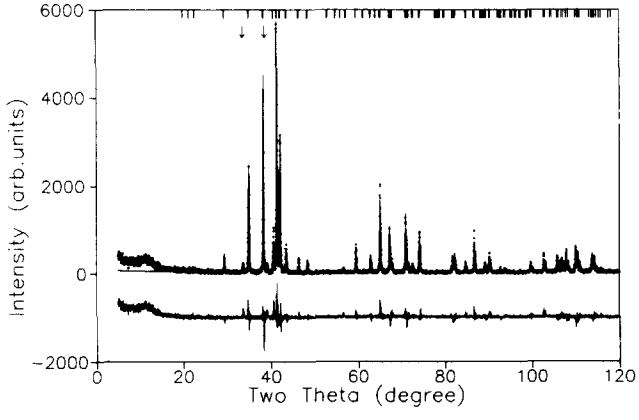

Fig. 1. X-Ray powder diffraction diagram of $ZrCr_2$ at room temperature. The vertical bars at the top of the plot represent the positions of the Bragg diffraction lines of the refined C14 type of Laves phase structure. The arrows represent the positions of the superstructure reflections. The curve at the bottom of the plot is the difference between the measured and calculated patterns.

It was verified that the two peaks are not due to any other possible compound such as unreacted zirconium or chromium or oxides but are due to superstructure reflections, namely the 015 and 113 reflections of one hexagonal lattice with doubled c axis, such as the C36 Laves phase structure.

Laves phases are layered structures and extensive studies on these have been carried out by Komura [12], Kitano et al. [13] and Frank and Kasper [14,15]. Following the notation of Komura [12], there are six types of layers denoted A, B, C, A′, B′, C′ which can be stacked in different ways. Each layer consists of four planes of atoms, with two planes composed of zirconium atoms and the other two of chromium atoms. The planes in a layer are always stacked in an intercalated configuration. Only two types of layer-stacking sequence are allowed, the h (hexagonal) and c (cubic) sequences, and this results in three types of fundamental structure: a two-layer structure with the hh sequence (C14 Laves phase), a three-layer structure with the ccc sequence (C15 Laves phase) and a four-layer structure with the hchc sequence (C36 Laves phase). However, other types of ordered structure can also arise when there is a repeated stacking pattern of a combination of h and c sequences. For example, Komura [12] identified a nine-layer structure with the hhc sequence and a five-layer structure with the ccchh sequence in the MgCuAl

Table 1
Refined $ZrCr_2$ and $ZrCr_2H_3$ structure parameters at room temperature. Space group $P6_3/mmc$

Atom	Position	Coordinates	Cell parameters
$ZrCr_2$			
Zr	4*f*	$z = 0.0603(3)$	$a = 5.103(2)$
Cr1	2*a*		$c = 8.268(4)$
Cr2	6*h*	$x = 0.8317(9)$	
$ZrCr_2H_3$			
Zr	4*f*	$z = 0.065(1)$	$a = 5.342(2)$
Cr1	2*a*		$c = 8.731(4)$
Cr2	6*h*	$x = 0.836(4)$	

system. These phases appear to be mixed with the predominant C36 phase in this compound. Diffuse X-ray scattering in MgCuAl, coming from other more randomly stacked sequences, has also been observed and characterized by special X-ray techniques [12,13].

It appears that the presence of stacking sequences other than the predominant hh sequence is also the case in the $ZrCr_2$ compound for the following reasons. (1) The reflections at $2\theta = 33.67°$ and 38.71° (arrows in Fig. 1) exist only for structures whose number of layers is greater than or equal to four. (2) For these reflections to have some diffracted intensity, c and h sequences must be allowed to be present in the structure. For example, in cases where only c sequences or only h sequences are present, these reflections have zero intensity, but in the case of an hchc sequence the 015 reflection is particularly strong.

A trial fitting of the X-ray diffraction pattern with a mixture of phases, namely C14 and C36, resulted in annihilation of the phase other than the C14. Other stacking sequences have been tried in the refinement, such as the nine- and five-layer structures mentioned above, as well as the hhhc, hhhhc, etc., but no improvement in the refinement was achieved. These alternative stacking sequences were simulated by referring to a structure whose space group is $P3$ and by which all the Laves phases can be constructed by stacking planes of atoms layer by layer. However, not all the sequences can be simulated, because the number of layers needed becomes too large and cannot be handled in the computer routine, since the number and density of reflections increase accordingly. For example, the hhc sequence needs nine layers in order to complete one cycle, whereas the hhhhc needs 15. Moreover, stacking with a large number of h sequences between isolated c sequences can also result in a non-uniform stacking, i.e. a variable number of h sequences between each c sequence.

A complete identification of these phases is difficult with the trial method mentioned above and the special electron and X-ray microscopy techniques utilized by Kitano et al. [13] and Komura [12] could be useful for this purpose. Thus what can be concluded is that the $ZrCr_2$ compound is mainly formed by the hexagonal C14 Laves phase mixed with unresolved and possibly ordered phases with unknown stacking sequences.

The density of defects is difficult to compute but can be estimated by the ratio between the intensities of the peaks at $2\theta = 33.67°$ and 35.01° in Fig. 1, respectively from the 015 reflection of the C36 structure and from the 110 reflection of the C14 structure. Taking into account the respective structure factors and the multiplicity of these reflections, it was estimated that about 5% of the compound has defects. This means that on average one c sequence is encountered after every 20 h layer sequence. It should be noticed, however, that the estimate was made with the assumption that the defects have the same diffracted intensity as the 015 reflection of the C36 type of structure, which happens to be very strong. Isolated c sequences diluted in h sequences can diffract with lower intensity, since two or more contiguous layers with the c sequence, as with the h sequence, do not contribute to this reflection. Thus the estimated density of defects should be taken as a lower limit.

4. TDPAC results

The TDPAC of γ rays, among other features, can detect an electric field gradient (EFG) acting on a radioactive nucleus by means of the interaction of the EFG tensor with the nuclear quadrupole moment (Q) of the probe nucleus. Two γ rays from the 133–482 keV cascade of excited ^{181}Ta, populated from the β-decay of ^{181}Hf diluted in the samples, were detected by two BaF_2 detectors. The coincidence counts were registered as a function of the time elapsed between the emission of the two radiations (time resolution about 1 ns). During this time the ^{181}Ta nucleus is in its intermediate $\frac{5}{2}$ spin state (10.8 ns half-life) and is perturbed by the environmental EFG which induces transitions between its magnetic substates. The coincidence-counting rate, without time resolution effects, is given by [16]

$$W(\theta, t) = W_0 \exp\left(\frac{-t}{\tau}\right)\left(1 + \sum_k A_{kk} G_{kk}(t) P_k(\cos\theta)\right)$$

where W_0 is a constant which depends on the geometry and efficiency of the detectors, τ is the mean lifetime of the intermediate state of the probe nucleus, A_{kk} are the (known) unperturbed angular correlation coefficients, $G_{kk}(t)$ are the perturbation factors, $P_k(\cos\theta)$ are Legendre polynomials and θ is the angle between the detectors. Knowing that only A_{22} and A_{44} terms appear for the case of ^{181}Ta and that $A_{44} \ll A_{22}$, and taking measurements at $\theta = 90°$ and 180°, the perturbation factor is extracted by determining the ratio

$$A_{22}(t) = A_{22} G_{22}(t) \approx \frac{-2[W(180, t) - W(90, t)]}{W(180, t) + 2W(90, t)}$$

The EFG main component V_{zz} and its asymmetry parameter $\eta = (V_{xx} - V_{yy})/V_{zz}$ are determined by a least-squares fit of the data with the equation

$$G_{22}(t) = \sigma_{20} + \sum_{n=1}^{3} \sigma_{2n} \cos(\omega_n t) \quad (1)$$

where the coefficients σ_{2n} and frequencies ω_n are known functions of the asymmetry parameter η of the EFG and of the quadrupole frequency [17]

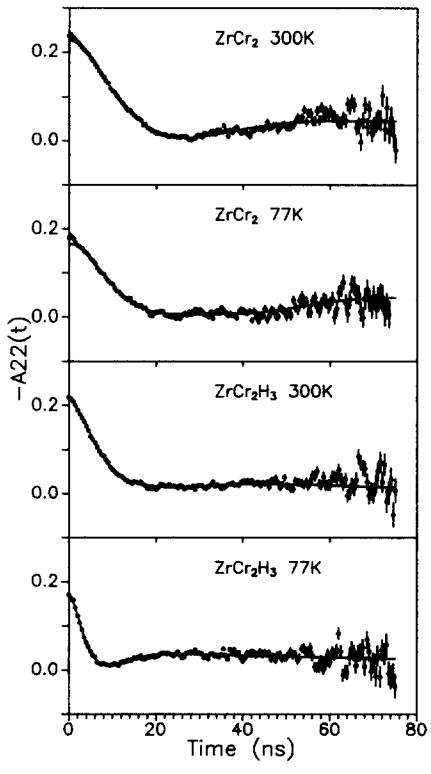

Fig. 2. TDPAC spectra of $ZrCr_2$ and $ZrCr_2H_3$ measured at 77 and 300 K.

$$\omega_Q = \frac{eQV_{zz}}{4I(2I-1)\hbar}$$

As usual, Q is the electric quadrupole moment of the nucleus in its intermediate state and I is its total angular momentum. The effects of the time resolution τ_R and the width of the distribution of the EFG, δ, are conveniently introduced by multiplying the terms of Eq. (1) by the exponential functions [18,16] $\exp(-\omega_n^2\delta^2t^2/2)$ and $\exp(-\omega_n^2\tau_R^2/2)$.

TDPAC spectra of $ZrCr_2$ and $ZrCr_2H_3$ measured at 300 and 77 K are shown in Fig. 2. The points in these figures are experimental values of the perturbation factor, while the solid curves represent the fits of Eq. (1) by the least-squares method. In all cases only one type of probe site was sufficient to obtain a good fit to the data, but large frequency distributions were observed.

5. Discussion

5.1. The $ZrCr_2$ compound

As can be seen in Fig. 2, the angular correlations are perturbed in all cases and this was attributed to the $3m$ point symmetry of the sites occupied by the Ta probes. Within experimental error, the mean quadrupole frequency and asymmetry parameter for $ZrCr_2$ are the same at 77 and 300 K, being respectively $\omega_Q = 9.7 \pm 0.4$ Mrad s^{-1} and $\eta = 0.62 \pm 0.04$.

A striking feature of these results is the large width δ of the EFG distributions, namely $\delta = 0.55$ and 0.79 respectively for $T = 300$ and 77 K. This effect does not decrease even after annealing for up to 6 days at 1073 K. It is very improbable that this effect comes from large lattice imperfections such as vacancies or dislocations, since the X-ray results presented in Fig. 1 show only narrow peaks whose widths are of the order of the resolution of the instrument. Similar observations have also been made in other studies of Laves phases with the cubic C15 structure [19,20], suggesting that this is a common feature of these layered compounds.

The result can be understood if these large distributions are ascribed to the stacking faults detected by X-ray analysis of the $ZrCr_2$ compound. In fact, looking at the immediate vicinity around the Zr atoms, it is found that there are two types of Zr site, one being the normal $3m$ point symmetry site of a $P6_3/mmc$ structure and the other coming from the stacking defects. To illustrate this point, a Friauf polyhedron [5] which represents the smallest building block of the structure of the Laves phase family is shown in Fig. 3. The polyhedron consists of four triangular and four hexagonal faces, the Zr atom being located at the centre of the polyhedron and the Cr atoms at the vertices. Four additional Zr atoms, not shown in the figure, are located outside each of the hexagonal faces [5] and are also at the centres of their respective and similar polyhedra.

Outside three of the four triangles we have a chromium atom at a distance of 4.689 Å from the centre, while at the outside of the fourth triangle there is a zirconium atom at 5.130 Å from the center. The three triangles of the Friauf polyhedron which have a chromium atom in front of them are somewhat deformed,

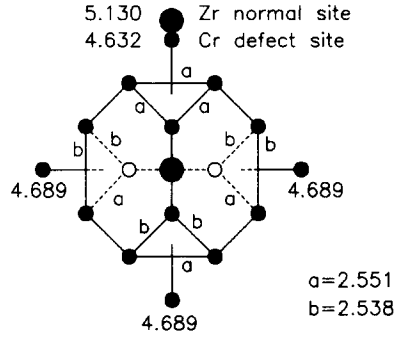

Fig. 3. Atomic configuration around a Zr atom in the $ZrCr_2$ structure with and without a stacking defect. Large and small circles represent respectively Zr and Cr atoms. The numbers represent distances in angstroms of the corresponding atoms from the centre of the Friauf polyhedron or the lengths of the labelled edges. The two close atoms shown at the top are mutually exclusive: in a perfect lattice only the Zr atom is present, while in a defect the site is occupied by the Cr atom at the quoted distance from the centre.

since two of their sides have a length of 2.538 Å while the remaining side is 2.551 Å in length. In contrast, the triangle with a zirconium atom placed at the outside is regular with sides of 2.551 Å. This triangle is shared with other adjacent Friauf polyhedra. The point symmetry of the Zr sites is $3m$.

It can be verified that when the zirconium atom of the centre of the Friauf polyhedron is located at a stacking fault (change from an ...hhhhh... sequence to an ...hchhh... sequence), the zirconium atom which was located at the outside of one of the triangular faces is substituted by a chromium atom at a distance of 4.632 Å from the centre. The change occurs by virtue of a shift of one plane of chromium atoms by $\pm\frac{1}{3}$ of the unit cell dimension in the $\bar{1}10$ direction [12] or, equivalently, by the substitution of one layer (A, B, C) by the corresponding primed layer (A′, B′, C′) or vice versa [13]. In this situation all four corners of the polyhedron have the same kind of atomic arrangement, the differences between these corners being only due to different sizes of the edges of the tetrahedra formed by the Cr atoms. It is, however, quite likely that the lattice will relax locally to a structure where all four corners of the polyhedron are equivalent and where the Zr site at the centre has $\bar{4}3m$ point symmetry as in the relaxed cubic C15 type of structure. This mechanism certainly introduces local strains in the structure which can propagate around the defect. It is then likely that a large number of atomic configurations might coexist, giving rise to a broad distribution of the EFG experienced by the Zr atoms.

5.2. The $ZrCr_2$ hydride

The pressure–composition–temperature measurements of Pebler and Gulbransen [21] on $ZrCr_2H_x$ showed that this hydride is a two-phase system for $x<3$. This agrees well with our X-ray analysis for $x=2$, where it was found that the system is composed of a hydrogen-free $ZrCr_2$ alloy and the $ZrCr_2H_{3.0\pm0.1}$ hydride. Thus only results for $x=3$ are shown here.

TDPAC measurements have been performed on $ZrCr_2H_3$ as a function of temperature in the range between 77 and 300 K, the results of which are shown in Fig. 2. Large EFG distributions have been observed for this case also. They are attributed to lattice imperfections instead of layer stacking defects as in the case of $ZrCr_2$, because wide peaks are also observed in the X-ray powder diffraction pattern of the hydride. We believe that these imperfections come mainly from a non-uniform distribution of hydrogen atoms among the available sites as well as from the presence of vacancies and dislocations introduced after the lattice expansion caused by the absorption of hydrogen.

Fig. 4 shows the temperature dependence of the quadrupole frequency and the width of the distribution

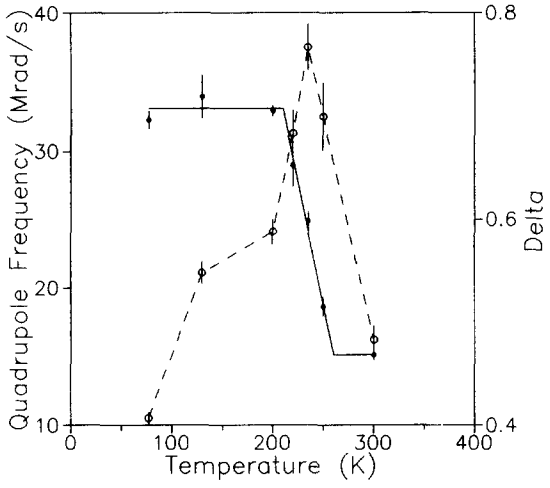

Fig. 4. Quadrupole frequency ω_Q (full circles) and width of the quadrupole frequency distribution, δ (open circles), as a function of absolute temperature for $ZrCr_2H_3$.

of the EFG for $ZrCr_2H_3$. The behaviour of the temperature dependence of the quadrupole frequency ω_Q indicates a phase transition at 230 K. As has been observed with other hydrides of Laves phases [19], this transition is relatively wide and for $ZrCr_2H_3$ ranges from 200 to 260 K. No hysteresis effect has been observed. At 300 K the quadrupole frequency ω_Q is 15.1 ± 0.3 Mrad s^{-1} and the asymmetry parameter η is 0.26 ± 0.05. Below the phase transition the quadrupole frequency and the asymmetry parameter of the EFG seem to be temperature independent. The measured values at 77 K are $\omega_Q=32.3\pm0.6$ Mrad s^{-1} and $\eta=0.43\pm0.05$.

Also shown in Fig. 4 is the temperature dependence of the width δ of the quadrupole frequency distribution. This width has a maximum at exactly the middle of the transition, thus clearly indicating that at $T=230$ K the $ZrCr_2H_3$ system is composed of a mixture in equal amounts of the two phases appearing individually above and below the transition. Each phase has its own mean quadrupole frequency with a relatively wide distribution; at the transition temperature these overlap to produce one large distribution. Above the transition temperature the structure of the metal lattice of the hydride is the same as that of the $ZrCr_2$ compound (see Table 1), whereas the low temperature structure is not yet established.

6. Conclusions

TDPAC and X-ray measurements on $ZrCr_2$ revealed an intrinsic defect in the crystal structure of the compound which was attributed to stacking faults after X-ray powder diffraction refinement and structure analysis in the vicinity of the Zr sites. Further studies are needed to reveal to what extent the density of these defects is dependent on the quantity of impurities in the samples,

such as oxygen or hafnium, or on the method of preparation. Although these defects obscure the observation of the effect of hydrogen atoms absorbed at low concentrations in this alloy with the TDPAC method, it was possible to observe a phase transition for the $ZrCr_2H_3$ hydride at 230 K. By analogy to compounds with similar structures [20], a phase transition is expected for $ZrCr_2$ at a temperature lower than 77 K. An indication in this respect has been obtained in this work from the observed width of the EFG distribution, which is larger for $T=77$ K than for $T=300$ K, pointing out the imminence of a phase transition.

Acknowledgements

The authors are grateful to the staff of the X-ray laboratory of the Instituto de Física e Química de São Carlos where the X-ray measurements were performed. One of us (J.M.F.) wishes to thank Professors A.K. Cheethan, R.B. von Dreele and R.A. Young for helpful discussions on the Rietveld method for structure analysis. W.P. was supported by a fellowship from CNPq. J.I.M. was supported by a fellowship from CAPES.

References

[1] Y. Fukai, *J. Less-Common Met., 101* (1984) 1.
[2] J.J. Didisheim, K. Ivon, D. Shaltiel and P. Fischer, *Solid State Commun., 31* (1979) 47.
[3] R. Hempelmann, D. Richter, O. Hartmann, E. Karlsson and R. Wäppling, *J. Chem. Phys., 90* (3) (1989) 1935.
[4] D. Shaltiel, *J. Less-Common Met., 73* (1980) 329.
[5] D.P. Shoemaker and C.B. Shoemaker, *J. Less-Common Met., 68* (1979) 43.
[6] W. Rostoker, *Trans. AIME, 197; J. Met., 5* (1953) 304.
[7] W.B. Pearson, *A Handbook of Lattice Spacings and Structures of Metals and Alloys,* Pergamon, London, 1958, p. 79.
[8] D. Fruchart, A. Rouault, C.B. Shoemaker and D.P. Shoemaker, *J. Less-Common Met., 73* (1980) 363.
[9] T. Riesterer, P. Kofel, J. Osterwalder and L. Schlapbach, *J. Less-Common Met., 101* (1984) 221.
[10] D.G. Ivey and D.O. Northwood, *J. Less-Common Met., 115* (1986) 295.
[11] D.B. Wiles and R.A. Young, *J. Appl. Crystallogr., 14* (1981) 149.
[12] Y. Komura, *Acta Crystallogr., 15* (1962) 770.
[13] Y. Kitano, Y. Komura and H. Kajiwara, *Acta Crystallogr. A, 36* (1980) 16.
[14] F.C. Frank and J.S. Kasper, *Acta Crystallogr., 12* (1959) 483.
[15] F.C. Frank and J.S. Kasper, *Acta Crystallogr., 11* (1958) 184.
[16] E. Karlsson, E. Mathias and K. Siegbahn, (eds.), *Perturbed Angular Correlations,* North-Holland, Amsterdam, 1964, Chap. 1.
[17] T. Butz, *Hyperfine Interact., 52* (1989) 189.
[18] R. Béraud, I. Berkes, J. Danière, G. Marest and R. Rougny, *Nucl. Instrum. Methods, 69* (1969) 41.
[19] R. Heidinger, P. Peretto and S. Choulet, *Hyperfine Interact., 15–16* (1983) 787.
[20] R. Heidinger, P. Peretto and S. Choulet, *Solid State Commun., 47*(4) (1983) 283.
[21] A. Pebler and E.A. Gulbransen, *Trans. Metall. Soc. AIME, 239* (1967) 1593.